Journal of Applied Fluid Mechanics, Vol. 12, No. 4, pp. 1177-1188, 2019.
Available online at www.jafmonline.net, ISSN 1735-3572, EISSN 1735-3645.
DOI: 10.29252/jafm.12.04.29537

Effect of Property Variation on the Fluid Flow and Thermal Behavior in a Vertical Channel

K. Roy and B. Das†

Department of Mechanical Engineering, National Institute of Tecnology, Silchar, Assam, 788010, India

†*Corresponding Author Email: biplab.2kmech@gmail.com*

(Received August 16, 2018; accepted December 3, 2018)

ABSTRACT

Natural convection in a vertical fin array is studied numerically for Non-Boussinesq and Boussinesq fluid with the effect of property variations. Simulations are carried out for the specified range: non-dimensional fin spacing = 0.2 to 0.5, non-dimensional clearance = 0.05 to 0.4 and Grashof number = 1.86×10^5 to 8.64×10^5. Computations are executed to plot the isotherms contours across the section close to the outlet to exemplify the effect of non-Boussinesq fluid in natural convection for variable properties. Computation demonstrates a maximum of 9% higher overall Nu for fixed property Boussinesq fluid than compared to the non-Boussinesq fluid. And for the Boussinesq fluid with the thermo-physical property maintained constant, the results obtained for local Nusselt number is consistently higher than compared to the inconsistent thermo-physical property. Also temperature drop close to the tip of the fin is higher at higher Gr, indicating higher heat transfer rate. Finally, for overall Nusselt number a correlation with the governing parametyers for the present investigation is developed.

Keywords: Natural convection; Non-Boussinesq; Variable property; Nusselt number.

NOMENCLATURE

C	fin tip to shroud clearance
C^*	dimensionless fin tip to shroud clearance
Gr	Grashof number
H	fin height
k	thermal conductivity
L	fin length
Nu	overall Nusselt number
Pr	Prandtl number
Q	overall heat transfer
S	fin spacing
S^*	dimensionless fin spacing
T	temperature
t	fin thickness
W^*	dimensionless induced velocity
u,v,w	components of velocity in x,y and z directions
U,V,W	dimensionless velocity components in x,y and z directions
x,y,z	axial and cross stream coordinates
β	thermal volumetric expansion coefficient
θ	dimensionless
ϕ	viscous dissipation terms (not considered in the present investigation)
ΔT	scaling temperature difference

Subscripts

f	fin
l	local
o	ambient
w	wall

1. INTRODUCTION

An extensive use of finned surface to improve heat transfer in a wide range of engineering applications such as electronic and thermoelectric device cooling, solar energy, heat exchangers, air conditioning and many more. Study of natural convective heat transfer is significant, as in any kind of system it is ubiquitous. Available literature has shown that immense numbers of numerical and experimental studies on free convection heat transfer from finned surface are carried out.

Yüncü and Anbar (1998) experimentally investigated natural convective heat transfer from rectangular shape finned set-up on a horizontal base. The significance of fin spacing, fin height, clearance and temperature difference in natural convection heat transfer is investigated for fins on a horizontal

base by Guvenc and Yuncu (2001) and Arquis and Rady (2005). Also importance of new horizontal design on natural convection by using short length, pin fins along with plated fins in a row-wise arrangement and cross plated fin pattern by Dialameh *et al.* (2008), Haghighi *et al.* (2018) and Feng *et al.* (2018) respectively. Huang and Wong (2012) numerically studied the unsteady behavior with increasing fin length that causes decrease of average convection heat transfer coefficient. The importance of natural convection in a mixed convection is presented by Dogan and Sivrioglu (2012) for vertical fin array kept on a horizontal base at the entry region.

There exists literature (Starner and McManus, 1963; Welling and Wooldridge, 1965; Harahap and McManus, 1967; Leung *et al.*, 1985; Karki and Patankar, 1987; Fisher and Torrance, 1999; Al-Sarkhi *et al.*, 2003; Yazicioglu and Yuncu, 2007) particularly investigating complete natural convection in a vertical fin array for a maximum rate of heat transfer, considering proper geometric parameters. For mixed convection Giri and Das (2012) studied at the entry region of shrouded vertical fin arrays rectangular shape placed over the vertical base plate by decoupling the velocity entering into two elements, first velocity of the fan and second the buoyancy causing induced velocity. They further extended the numerical investigation on mixed convection in presence of vortex generator (i.e., Das and Giri, 2015). Also, Goshayeshi *et al.* (2011) numerically analyze natural convection for developing and developed enlarged hydrodynamic and heating parts of the vertical fin array. Some improvisations on the shape and other conventional geometric parameters of vertical channel have been investigated. Lee *et al.* (2016) considered triangular fins on a vertical cylinder and developed a correlation for Nusselt number. Chang *et al.* (2017) studied numerically the natural convection heat transfer for a set of vertical fin arrays with/without dimples. Also, natural convective heat transfer analyzed numerically by Pathak *et al.* (2018) for a vertical variable height fin array but the detail effect of property variation is not discussed.

Although a lot of investigations have been done on free convective heat transfer, only a handful of literature discusses the effect of properties variation on natural convection heat transfer. In late 1999, Emery and Lee (1999) highlighted the effects of property variations with significant flow pattern change in a square enclosure. Also, Li *et al.* (2007), and Reddy *et al.* (2010) presented the results of the convection heat transfer while dealing with non-Boussineśq fluid for a micro channel heat sink and centrally located vertical heat generating rod respectively. Zhang and Cho (2018) presented the effect of the non-Boussineśq fluid and the scheme of descending isotherms in horizontal annulus geometry for natural convection. For mixed convection, the effect of property variation for non-Boussineśq fluid is investigated by Das and Giri (2014). Thus, the present investigation solves a problem on the effect of property variation on natural convection along with the comprehensive investigation of the fin spacing and clearance between the adiabatic shroud and fin tip is presented for vertical fin array configuration. It also incorporates a detailed analysis of results for Grashof number variations, as no literature is available on the effect of property variation for a shrouded vertical fin array this analysis makes a significant contribution. Range of the temperature applied in the present article is further associated with the flat plate solar air collector and heat transfer of other similar components. Physical configuration is reported next.

2. PROBLEM DESCRIPTION AND FORMULATION

2.1 Physical Configuration

Physical configuration of the present investigation is presented in Fig. 1(a). All rectangular vertical fins are placed over a base plate, which is kept vertical and at a high temperature. Three sets of inter-fin spacing '*S*' is kept constant throughout. Also fin length '*L*' and thickness '*t*' is kept constant with respect to three set of fin height '*H*'. The adiabatic shroud is arranged uniformly over all the fin tips at distance of clearance '*C*' in between them. For the present investigation five clearance '*C*' values are considered. Each duct is of identical rectangular shape, composed of two successive fins, shroud and the base. Acquired dimension of the duct is $L\times S\times(H+C)$. The top view of the cross section is presented in Fig. 1(b). The base and fins are of same material. The vertical base and left side fin forms a corner, where the position of the origin is considered for the coordinate system. The *x*-, *y*- and *z*- direction are directly parallel to the base, height and length of the fin respectively. As the problem setup is considered to be vertical. Arrangement of the vertical insulated shroud over the fin tip with a clearance of '*C*' shows a chimney effect. In the vertical shrouded fin array natural convective upward flow is due to a temperature difference between the higher temperature (T_w) for the base maintained uniformly and the ambient temperature (T_o). The mathematical model for the present investigation is elucidated next.

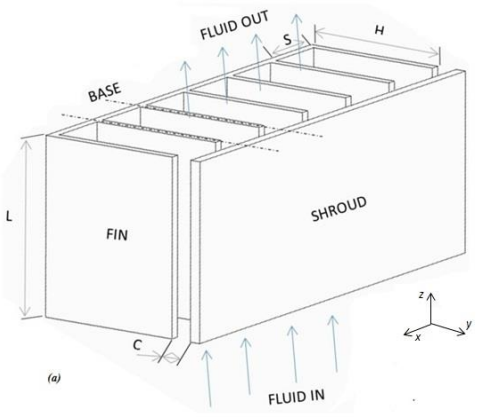

Fig. 1(a). Rectangular shaped fins placed over a vertical base plate.

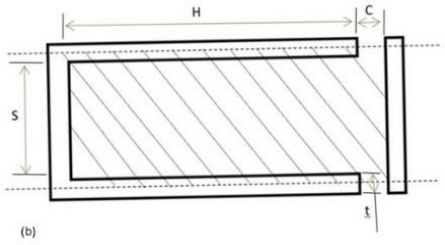

Fig. 1(b). Cross section view for one of the symmetric flow passages.

2.2 Mathematical Formulation

The governing equation in the present problem is mathematically formulated using the equations of conservation of mass, momentum and energy. The air flow is considered to be steady, laminar and incompressible caused by the less value of the flow velocity. Negligible stream wise diffusion is considered due to the dominance of the stream wise convection. Here, p represents total pressure defect (i.e., $p = p_o - p_s$), where, p_o is the hydrostatic pressure and p_s is the static pressure. Also an average pressure defect

$$p_{avg} = \left(\int_0^{H+C} \int_0^{0.5S} p(x,y,z)dxdy \; / A_c \right)$$

which varies with z and is the spacewise varying pressure which is a function of x, y, and z. As the case is for parabolic flow, where dp_{avg}/dz is generally much higher than dp'/dz and thus the dependence on z-direction of the cross-stream pressure can be neglected:

$$p(x,y,z) = p_{avg}(z) + p'(x,y,z)$$

For the present vertical setup problem at the gravity force term in the z-momentum equation, the Boussineśq approximation is considered i.e.,

$$\rho = \rho_o \left[1 - \beta (T - T_o) \right]. \tag{1}$$

The aforesaid physical configuration may be elucidated mathematically by following equations:

Equation of continuity

$$\frac{\partial u}{\partial x} + \frac{\partial v}{\partial y} + \frac{\partial w}{\partial z} = 0 \tag{2}$$

Equation of x-momentum

$$\rho \left(u\frac{\partial u}{\partial x} + v\frac{\partial u}{\partial y} + w\frac{\partial u}{\partial z} \right) = -\frac{\partial p'}{\partial x} + \mu \left(\frac{\partial^2 u}{\partial x^2} + \frac{\partial^2 u}{\partial y^2} + \frac{\partial^2 u}{\partial z^2} \right). \tag{3}$$

Equation of y-momentum

$$\rho \left(u\frac{\partial v}{\partial x} + v\frac{\partial v}{\partial y} + w\frac{\partial v}{\partial z} \right) = -\frac{\partial p'}{\partial y} + \mu \left(\frac{\partial^2 v}{\partial x^2} + \frac{\partial^2 v}{\partial y^2} + \frac{\partial^2 v}{\partial z^2} \right). \tag{4}$$

Equation of z-momentum

$$\rho \left(u\frac{\partial v}{\partial x} + v\frac{\partial v}{\partial y} + w\frac{\partial v}{\partial z} \right) = -\frac{\partial p_{avg}}{\partial y} + \mu \left(\frac{\partial^2 v}{\partial x^2} + \frac{\partial^2 v}{\partial y^2} + \frac{\partial^2 v}{\partial z^2} \right) + \rho\beta (T - T_o) g. \tag{5}$$

Equation of energy

$$\rho C_p \left(u\frac{\partial T}{\partial x} + v\frac{\partial T}{\partial y} + w\frac{\partial T}{\partial z} \right) = k \left(\frac{\partial^2 T}{\partial x^2} + \frac{\partial^2 T}{\partial y^2} + \frac{\partial^2 T}{\partial z^2} \right) + \varphi \tag{6}$$

Equation of fin conduction

$$\left(\frac{\partial^2 T}{\partial x^2} + \frac{\partial^2 T}{\partial y^2} + \frac{\partial^2 T}{\partial z^2} \right) = 0 \tag{7}$$

2.3 Inlet and Boundary Conditions

For negligible diffusion and dominating convection, the governing equations in z-direction become parabolic and before moving towards the solution, inlet condition is required to be mentioned. As the present problem is of free convection, the inlet stream wise velocity is not-known. The entry and exit pressure defect is assumed to be zero since the buoyancy is the driving force in natural convection. A guessed value is applied to estimate the inlet velocity in the present investigation. Ambient temperature is allocated to the inlet temperature and considered the cross stream velocity to be zero. When the pressure defect at the exit is zero, the initially assumed inlet velocity is considered to be free from error.

No-slip and impermeable conditions are considered to be at the base. Zero velocities and zero normal gradients of temperature up to the fin tip are considered at the symmetry plane passing through the fin. Above the fin height in between the fin tip and the shroud i.e., in the clearance zone normal velocity, temperature and normal gradients of the still existing velocities are considered to be zero. The fin base is kept at the temperature of the base plate and tip of the fin is made to be insulated. Also the shroud is assumed to be adiabatic, solid and impermeable surface. Mathematically, conditions of the boundary are mentioned as follows:

At the vertical base, i.e., ($0 \le x \le 0.5S$, y=0, $0 \le z \le L$)

$$u = v = w = 0, \;\; T = T_w \tag{8}$$

At the symmetry plane, which passing through the fin of height (H)

$$x = 0, \; 0 \le y \le H, \; 0 \le z \le L$$

$$u = v = w = 0, \;\; \frac{\partial T}{\partial x} = 0. \tag{9}$$

In the area $x = 0, \; H < y \le H + C, \; 0 \le z \le L$

$$u=0,\ \frac{\partial v}{\partial x}=0,\frac{\partial w}{\partial x}=0,\frac{\partial T}{\partial x}=0. \tag{10}$$

At the shroud i.e., $0\le y\le \mathrm{S},\ y=H+C, 0\le z\le L$

$$u=0,v=0,w=0,\frac{\partial T}{\partial y}=0. \tag{11}$$

Condition of fin boundary

$$y=0,\ T=T_w,\ y=H,\ \frac{\partial T}{\partial y}=0. \tag{12}$$

2.4 Coefficient of the Overall Heat Transfer and Overall Nusselt Number

To know the overall heat transfer rate is absolutely necessary to design or construct any heat transfer equipment. When the bulk temperature varies, it is difficult to enumerate the actual heat transfer rate. Calculation of the total heat transfer (Q), average heat flux (q), coefficient of overall heat transfer (h), and overall Nusselt number (Nu) is formulated mathematically, according to the temperature difference between the ambient and the base are as follows:

$$Q=Q_{fin}+Q_{base}$$
$$=\left(\int_0^L\int_0^H k\left.\frac{\partial T}{\partial x}\right|_{x=0} dydz\right)+\left(-\int_0^L\int_0^S k\left.\frac{\partial T}{\partial x}\right|_{y=0} dxdz\right) \tag{13}$$

$$q=\frac{Q}{(2H+S+t_f)L},\ h=\frac{q}{T_w-T_o}, \tag{14}$$

$$Nu=\frac{1}{(1+S)L}\int_0^L\left[\int_0^1\left.\frac{\partial T}{\partial x}\right|_{x=0} dy-\int_0^S\left.\frac{\partial T}{\partial y}\right|_{y=0} dx\right]dz \tag{15}$$

3. COMPUTATIONAL AND VALIDATION METHOD

The ultimate goal is to satisfy the continuity equation in order to evaluate a pressure field by using various numerical schemes. For the current problem, the pressure velocity coupling is resolve by using numerical SIMPLER algorithm explained by Patankar (1980). In the stream-wise coordinate backward difference scheme is used for the convective term. And on a staggered mesh the combined convective and diffusive terms of cross stream coordinates are discretized using the power-law scheme. The remaining diffusive terms are discretized using the central difference scheme. For every axial segment adequate number of outer iteration are considered as an iterative implicit method. The iteration is complete when the required convergence is obtained. Tri-diagonal matrix algorithm (TDMA) is used to solve the equation in a sequential form. Appropriate under relaxation factors are applied in order to minimize the possibility of deviation in the results due to computational errors; it also increases the stability and accuracy of the solution. In all the three directions, rectangular shaped grids are generated. Also close the inlet zone non-uniform grids are generated in the stream-wise direction (i.e., z-direction) to study variations of the boundary layer development. To solve the aforementioned problem a computational code developed by Giri and Das (2012) is applied with certain improvements.

3.1 Test For Grid Independence

A grid independence test is conducted for S^*= 0.3 with the combinations of grid sizes (X×Y×Z) is 28×38×140, 30×40×140 and 32×42×140. Also for S^*=0.5 it is 32×38×140, 34×40×140, and 38×46×140. *Z*-direction is the main flow direction. The grids are arranged in a geometric progression of increasing order. To show the accuracy of the present investigation, the solutions of various grid combination examinations are shown in Table 1.

Table 1 Grid independence examination

Non-dimentional fin spacing (S^*)	Grid Size (X ×Y × Z)	Overall Nusselt Number (Nu)
0.3	28 × 38 ×140	6.1673
	30 × 40 ×140	6.1682
	32 × 42 ×140	6.1701
0.5	32 × 38 ×140	6.6087
	34 × 40 ×140	6.6095
	38 × 42 ×140	6.6106

3.2 Validation Test

To validate the present investigation four sets of fin height and fin spacing are taken at three temperature differences from the experimental data of Starner and McManus (1963), numerical results are observed as shown in Fig. 2. These four sets values are used in the computation to find the convection coefficients particularly for a vertical setup with the difference of base and ambient temperatures. Results find favorable agreement with each other.

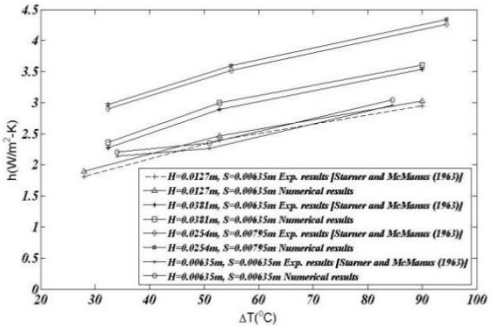

Fig. 2. Validation of the numerical code.

4. RESULTS AND DISCUSSION

Following geometrical and physical specifications are considered: Fin length is 0.5 m; fin heights are 0.03 m, 0.04 and 0.05 m; thickness of the fin is maintained to be 0.001 m. Dimensionless clearance distance between the fin tip and the shroud varies from 0.05 to 0.4 Also the non-dimensional fin

spacing are 0.2, 0.3 and 0.5. The fin conductivity is chosen to be 150 W/m-K. The ambient temperature (T_o) and the wall/base temperature of fin array (T_w) is assigned with a temperature of 20 °C and 100 °C respectively. The Prandtl number is considered to be of 0.7. The working fluid is air. Grashof number values of the current investigation are ranged from 1.86×10^5 to 8.64×10^5. The properties of the fluid are calculated at mean of ambient and base temperature. By assuming variable properties of the fluid, the authentic simulations are made. Also evaluation of dimensionless physical parameters of variable properties is made to compare with the fixed property results at the mean temperature. As suggested by Das and Giri (2014) the air properties are evaluated from the Eqs. (17) - (19) mentioned below:

Air Thermal Conductivity:

$$k = \frac{1.195\times10^{-3}(T)^{1.5}}{118+T} \tag{16}$$

Air Viscosity:

$$\mu = \frac{1.4888\times10^{-6}(T)^{1.5}}{118+T} \tag{17}$$

Air Density:

$$\rho = \frac{21.955\times28.93}{1.8(T-273.26)+491.69} \tag{18}$$

where, T is in Kelvin scale.

4.1 Effect of Boussinesq and Non-Boussinesq Fluid With Variable Properties

For the lucidity of the result, the cross-section of the base-fin arrangement with corresponding isotherms across the section close to the outlet (Z = 11.3) is presented in Fig. 3(a-f) and to exemplify the effect of non-Boussinesq fluid with the variable property. In the present figures, a comparison between contours of the Boussinesq approximation with non-Boussinesq fluid with inconsistent and consistent property is made by maintaining the same contour level. An isotherm is basically a line that joins points that have the same or equal temperature. And as we move away from the y- axis in the x- axis direction a decrease in each isotherm value is observed. For S^* = 0.2, the region of each isotherm contour lines is comparatively more than that of higher dimensionless spacing (i.e., S^* = 0.3). Also for S^* = 0.2 the value obtained for the isotherm is higher which means less heat transfer than that of S^* = 0.3, which directly justifies that the higher non-dimensional fin spacing generally causes higher heat transport also mention by Karki and Patankar (1987). Particularly when comparing Boussinesq fluid with non-Boussinesq fluid (i.e., Fig. 3(a-b) with Fig. 3(c-d)) it is observed to have similar trends but the values of the isotherm are marginally low. Figures 3(e-f) presents the effect of non-Boussinesq variable fluid density and variable thermal conductivity. These contour plots show similar trends but significantly the isotherm line values are lower for non-Boussinesq variable fluid density than that of variable thermal conductivity which implies higher heat transport for non-Boussinesq variable fluid density. Thus, the mass flow rate is also more for non-Boussinesq variable fluid density than that of variable thermal conductivity, keeping other properties constant.

Attention may now be turned to the specific impact of inconsistent thermo-physical parameters, such as density, viscosity, and conductivity on the overall Nusselt number (i.e., to indicate the heat transfer). The values of overall Nusselt number are presented in Table 2, for S^* = 0.2, 0.3, and 0.5. The density is varied with the fluid temperature at fixed constant thermal conductivity and viscosity. For S^* = 0.2, Boussinesq fluid with fixed property is 9% higher overall Nu than the variable density. A similar increase of 6 and 6.5% is obtained for S^* = 0.3 and 0.5 respectively. This may be caused by the lower density when it is considered to be a variable than that of a Boussinesq fluid. These trends are also shown by Das and Giri (2014, 2015), but for a mixed convection problem.

Attempts are also made to investigate the effects of the variable fluid viscosity, keeping remaining properties as constant. It is observed that the heat transport decreases by an amount of 2 to 4%. For variable viscosity, the viscosity is less near the inlet as average temperature is more than that of the inlet temperature. At increased viscosity, the fluid flow is through less resistance causing a decreased flow of fluid over the base-fin plate than that of Boussinesq fluid with the fixed property.

It is also observed that the constant fluid viscosity and variable fluid conductivity for Boussinesq fluid results in 6 to 7% lower overall Nu, compared to that of a constant physical property for Boussinesq fluid. Due to the lower thermal conductivity at the inlet region, lower heat is transported by the fluid. Although, fluid thermal conductivity increases after some time away from the inlet region but the temperature difference between the base-fin systems and bulk fluid gets reduced. This results in the decrease in the driving force for natural convective heat transport. Thus, variable conductivity significantly minimizes the overall heat transport. Table 2 also presents the maximum deviation for S^*=0.5.

Table 2 Overall results of inconsistent properties compared with constant properties.

ρ	μ	k	Nu		
			S^* = 0.2	S^* = 0.3	S^* = 0.5
B	F	F	5.13	7.19	7.81
B	V	V	4.59	6.58	7.15
B	V	F	4.90	7.02	7.65
B	F	V	4.81	6.74	7.30
V	F	F	4.70	6.75	7.35
V	V	V	4.16	6.17	6.61
V	F	V	4.39	6.31	6.85
V	V	F	4.46	6.59	7.22

C^* = 0.15, Gr = 4.42×10^5.
[F=Fixed, V=Variable, and B= Boussinesq]

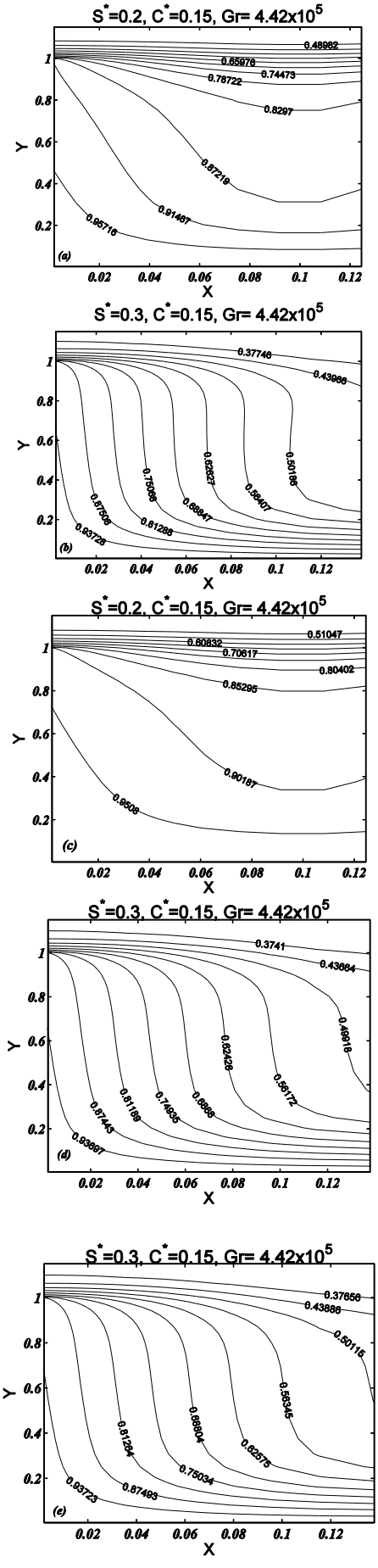

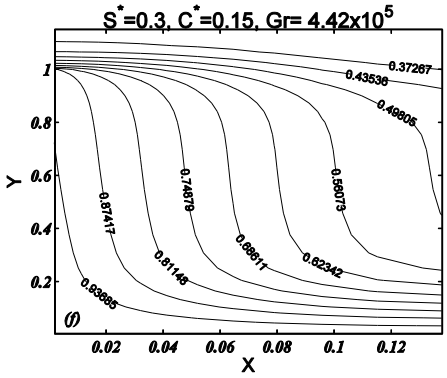

Fig. 3. Isotherms across the section at Z = 11.3, C^*=0.15, Gr=4.42×10^5, for constant property Boussinesq fluid (a) S^* = 0.2, (b) S^* = 0.3, for Non-Boussinesq fluid (c) S^*= 0.2, (d) S^* = 0.3, and for Non-Boussinesq fluid at S^* = 0.3 (e) k = variable, (f) μ = variable.

4.2 Variation of Pressure Drop

At three different non dimensional fin spacing (S^* = 0.2, 0.3 and 0.5), axial variation of average pressure P^* for Gr = 4.42×10^5 is shown in Fig. 5(a-b) for clearances (C^*=0.05 and 0.15). It is shows that P^* value tends to increase till a certain length along the increase in axial length, thereafter its value decreases. This trend is more prominent in the lower dimensionless fin spacing. Further, position of the maximum axial pressure tends to move towards the higher axial length for lower dimensionless fin spacing, indicating the contribution of more interfin circulation space. It is important to mention here that the non-dimensional pressure is elucidated in such a way that the lower the actual pressure higher will be the dimensionless pressure. Thus, initial increase in dimensionless pressure indicates lower actual pressure and this is due to reduction in external pressure with the increase in axial length. Moreover it is inferred from the figures that maximum P^* value decreases with increase in the clearance. This is because of the reduction in flow resistance causing higher mass flow rate of air. Thus, for lower fin spacing the maximum average axial pressure is more than that of higher fin spacing. A resemblance may be found from Karki and Patankar (1987) and Pathak *et al.* (2018) for constant and variable height fin array, respectively.

4.3 Induced Velocity

The development of induced velocity with respect to dimensionless clearance is shown in Fig. 6(a-c). The increase in clearance causes increase in induced velocity values, as it helps inducting more amount of fluid into the collector system. Also it shows that, induced velocity values increases with the increase in spacing between fins due to reduction in flow resistances for all clearances. Figures also present the effect of Grashof number on the magnitude of induced velocity. The main driving force in natural convection is buoyancy force which is directly proportional to the Gr. Increase in Gr directly increases the value of induced velocity and causes the increase in natural convection too. It is important to mention here that Gr in the present problem is

increased by increasing the height of the fin at a maintained temperature difference. Also the obtained range of induced velocity is found to be 100 to 270 at lower Gr (i.e., 1.86×10^5) and 200 to 450 at Gr (i.e., 4.42×10^5), for $S^* = 0.2$, 0.3 and 0.5. Thus, for a fixed temperature difference increasing the fin height will not only increase the heat transfer area but also will increase the true driving force.

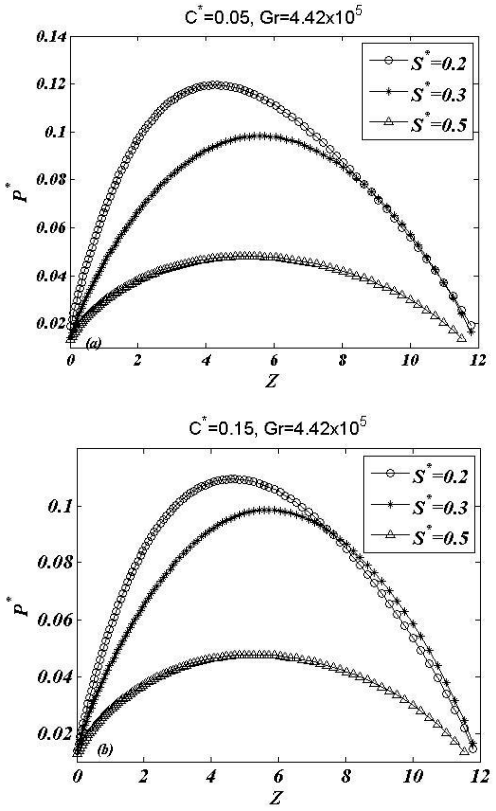

Fig. 4. Axial variation of average pressure for Gr= 4.42 × 10^5 (a) C^* = 0.05 and (b) C^* = 0.15.

4.4 Non-dimensional Bulk Temperature Distribution

Axial variation of non-dimensional bulk temperature in the fin array is potted in Fig. 7(a-c). An increase in the magnitude of θ_b is obtained, suggesting the fluids are thermally developing along the axial direction. It can be seen that with higher clearance more amount of fluid is inducted in the system and most of the fluid must be passing through the less resistive clearance zone, which causes lower magnitude of the bulk temperature near the exit. Attention may turn on to the effect of Gr increase. It is inferred from the figure that with the higher Gr value for same geometry, bulk temperature tend to decrease. The main reason is the combined effect of fluid flow bypass and increase in mass flow rate of air. Variation of dimensionless temperature with respect to the z direction in the plated finned array decreases on increasing Gr from 1.86×10^5 to 8.64×10^5 and is about 50 to 60% depending upon the clearance value. Similar, the effect of Gr is also mentioned by Dogan and Sivrioglu (2012), but for a mixed convective problem.

4.5 Variation of Fin Temperature

Fin temperature variation in *Y-Z* plane is illustrated in Fig. 8(a-c) for various Grashof number (i.e., from 1.86×10^5 to 8.64×10^5), for S^*=0.3 at C^*=0.15. Also, the effect of thermal conductivity is very less but cannot be neglected in case of natural convection. The increase in thermal conductivity decreases the temperature drop. As shown in Fig. 8(d-e), the variation of fin temperature is clearly observed for an increase in dimensionless fin spacing (i.e., S^* from 0.2 to 0.5). Natural convection heat transfer increases with the increase in temperature differences. For horizontal rectangular thick fins with short length similar observations are presented by Dialameh *et al.* (2008). Results indicate that higher temperature drop along the fin tip compared to that of the base, indicating the effect of fin conductivity; this is more prominent at the inlet. Further, it may be seen that temperature drop close to the tip of the fin is higher at higher Gr, indicating higher rate of heat transfer. Thus, for the present investigation it can be said that there is higher mass flow rate from the channel when the height of the fin is high.

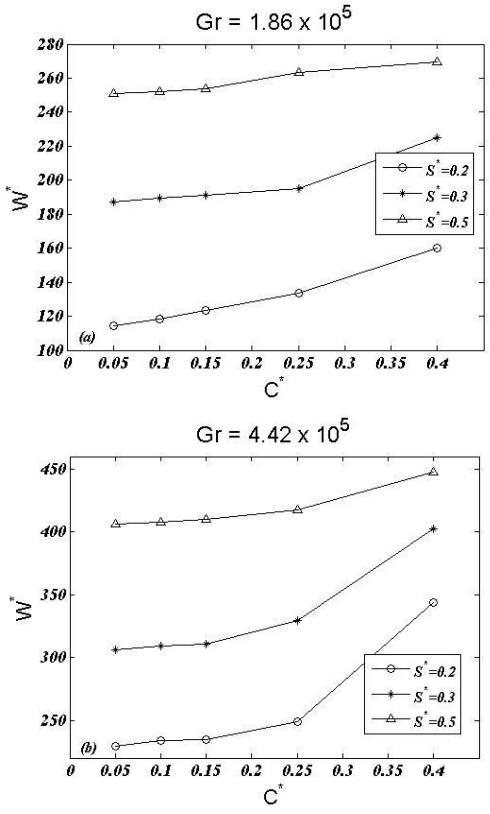

Fig. 5. Induced velocity plot at (a) Gr =1.86 ×10^5, and (b) Gr =4.42 × 10^5.

4.6 Local Nusselt Number

For clearance C^*= 0.15, the distribution of local Nusselt number with respective dimensionless fin spacing (i.e., S^* = 0.2, 0.3 and 0.5) is presented in Fig. 9(a-c). As buoyance force always act vertical upward, an increase in dimensionless fin spacing increases the local Nu value about 80 to 120%. Also with higher clearance a higher value of local Nu is

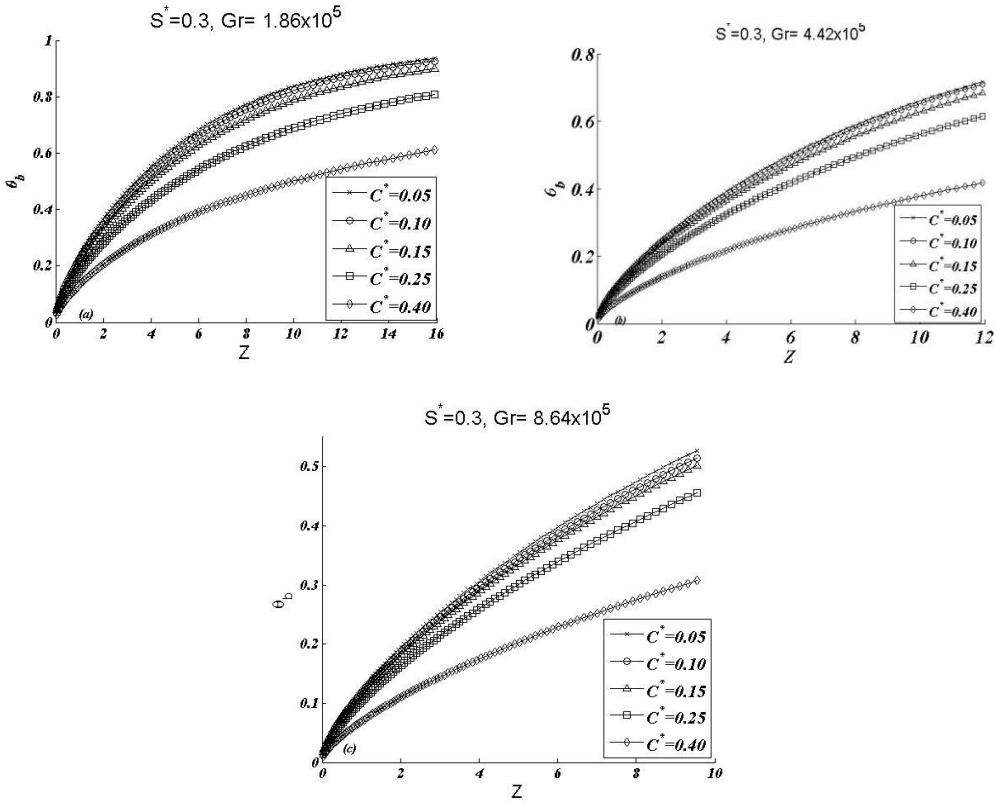

Fig. 6. Dimensionless bulk temperature variation for (a) Gr = 1.86 x 10^5, (b) Gr = 4.42 x 10^5 and (c) Gr=8.64 x 10^5.

obtained. The local Nu value is again more for increased Gr and particularly at S^* = 0.3, the local Nu observed to be increased by 150%, when Gr value is increased by about 365%. This trend is also mentioned by Li *et al.* (2007) that there is a substantial increment in the heat-transfer rate but results presented are for force convection.

4.7 Overall Heat Transfer and Fin thermal Efficiency

Overall heat transfer with dimensionless fin spacing is revealed in Fig. 10 at Gr = 4.42 × 10^5. Results reveal that heat transfer coefficient increases with the increase in spacing. The rate of increase is high till S^*=0.3, beyond which the rate is comparatively lower, and this is more prominent at lower Gr. At higher clearances the magnitude of heat transfer obtained is high, as illustrated from the induced velocity results. Further, overall heat transfer increases when the Gr value is increased from 1.86 × 10^5 to 8.64 × 10^5, and it is increased by about 250%. Results also reveal that C^* tend to increase the heat transfer. At Gr = 4.42 × 10^5 and S^*=0.3 maximum of 90% increase in heat transfer value is observed, when clearance is increased from C^*=0.05 to 0.4. This is justified as the cold fluid from the clearance zone move towards the interfin zone due to the buoyancy force and enhances the overall heat transfer. Attention may turn on to a significant indicator of fin heat transfer, which is its efficiency. In the present investigation, it is directly calculated from the deviation of actual fin heat transfer to isothermal fin heat transfer. Variation in fin thermal efficiency is presented in Fig. 11 at S^* = 0.3. A decreasing trend is observed for fin thermal efficiency with increase in Gr. And also interestingly higher efficiency is obtained for higher clearence.

4.8 Overall Nusselt Number

The variation of overall Nusselt number with Grashof number is plotted in Fig. 12(a-c). At a Gr = 1.86 × 10^5 and S^* = 0.3, increase in C^* from 0.05 to 0.4 increases the overall Nu value about 12% since the buoyance force is the vertical upward force and with increase in clearance flow resistance decreases. As the Gr approximates the ratio of the buoyancy to viscous force acting on the fluid, the density differences in the fluid occurring due to temperature gradients makes the Gr value directly responsible for a higher Nu value. Also, when dimensionless fin spacing is increased from 0.2 to 0.5 at Gr = 4.42 × 10^5 increase in overall Nu is maximum of about 70 to 90%. These trends are in good agreement with Li *et al.* (2007) and Das and Giri (2014).

Finally for the problem a correlation is developed for relating the overall Nusselt number with the governing parameters by using the computational data. The correlation is depicted in Fig. 12.

$$Nu^{-0.85}L^{*-0.1} = 0.24xxn^2 - 1.8xxn + 3.345 \qquad (19)$$

where $xxn = \left(S^{*0.205}C^{*0.027}Gr^{0.209}\right)^{0.5}$. The obtained correlation coefficient is 0.98. The relation is applicable for: $1.86\times10^5 \le Gr \le 8.64 \times 10^5$, $0.2 \le S^* \le 0.5$, $0.05 \le C^* \le 0.40$, and $0.05 \le L^* \le 0.40$.

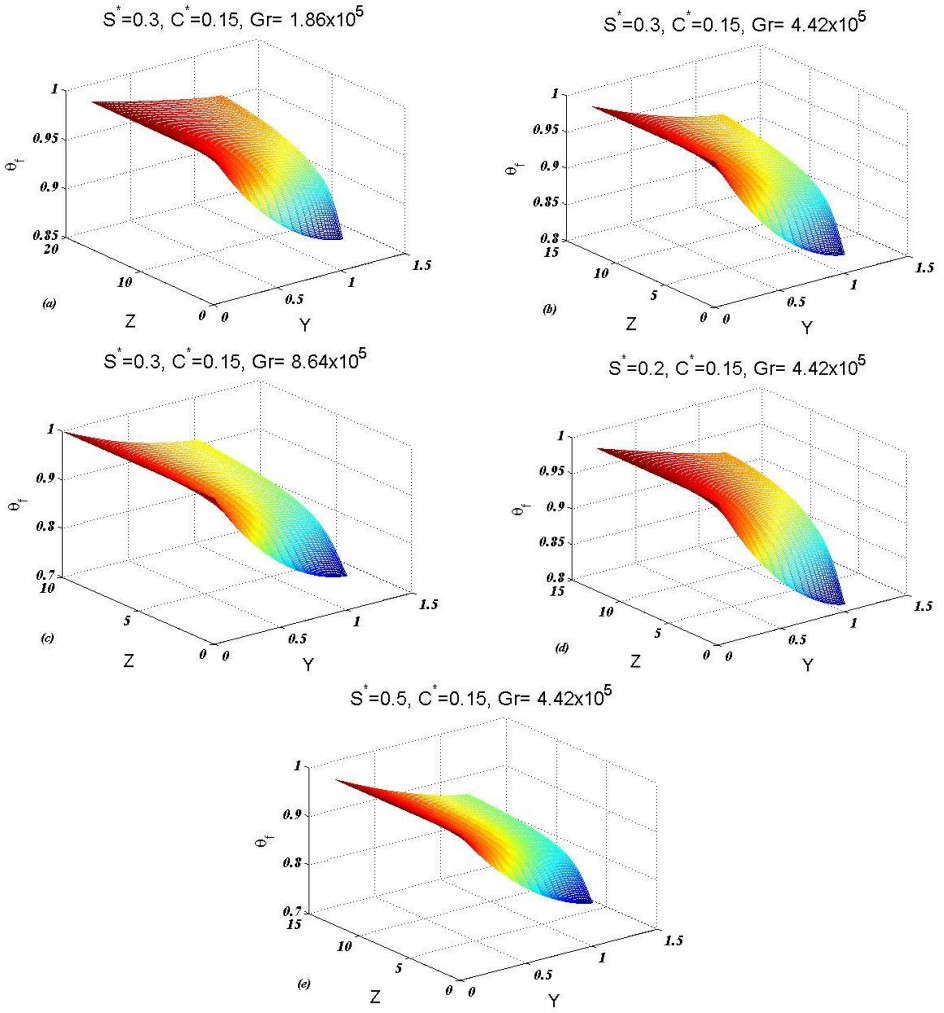

Fig. 7. Fin temperature variation for C^*=0.15 at (a) S^* = 0.3, Gr = 8.64 × 10^5, (b) S^*= 0.3, Gr =1.86 × 10^5, (c) S^* = 0.3, Gr = 4.42 × 10^5, (d) S^*= 0.2, Gr = 4.42 × 10^5 and (e) S^* = 0.5, Gr = 4.42 × 10^5.

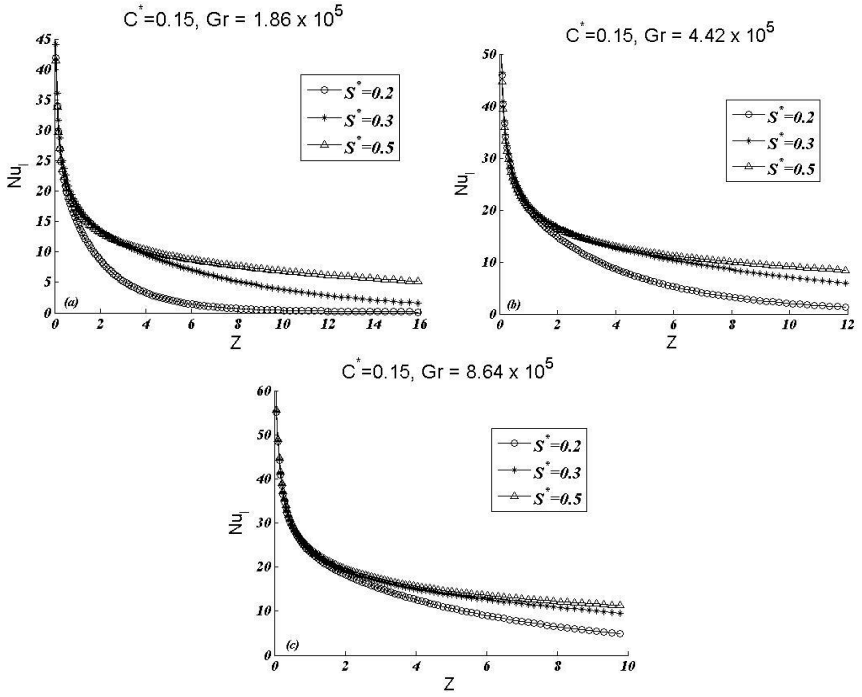

Fig. 8. Local Nusselt number variation for C^* = 0.15 at (a) Gr = 1.86 x 10^5, (b) Gr = 4.42 x 10^5 and (c) Gr = 8.64 x 10^5.

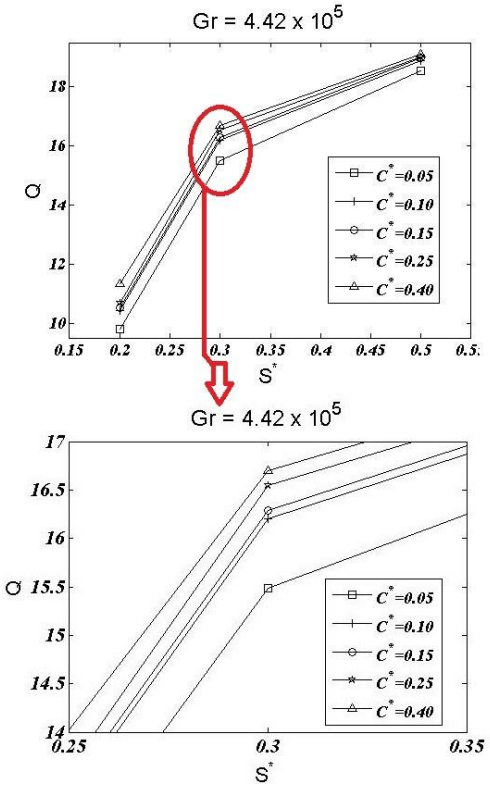

Fig. 9. Overall heat transfer variation for S^* = 0.2 to 0.5 at Gr = 4.42 × 10^5 along with maginfied plot.

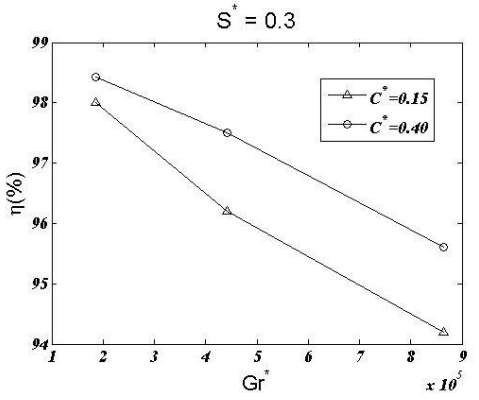

Fig. 10. Variation in fin thermal efficiency with Gr (1.86 × 10^5 to 8.64 × 10^5) at S^*=0.3 for C^*=0.15 and 0.40.

5. CONCLUSION

A numerical simulation is performed to analyze natural convection from a vertical fin array. The consequence of Non-Boussinešq fluid with inconsistent property on a vertical plated fin array configuration considered in the present investigation is highly significant for natural convection. For different non dimensional parameters, the solutions are obtained for clearance, fin spacing, Grashof number and fin height of the system. Computation yielded variation of Pressure, induced velocity, distribution of fin temperature and overall Nusselt number along with the effect of property variation. Following conclusions are drawn from the present investigation:

- Boussinešq fluid for fixed property obtained a maximum of 9% higher overall Nu than the variable density. And also with constant fluid viscosity and variable fluid conductivity for a Boussinešq fluid results about in 6 to 7% lower overall Nu value compared to that of a fixed physical property for Boussinešq fluid. Thus the effect of variable properties is significant for natural convection.
- For lower fin spacing the maximum average axial pressure is more than that of higher fin spacing. Increase in Gr directly increases the value of induced velocity and causes the increase in natural convection too. Dimensionless bulk temperature with respect to the z direction in the plated finned array decreases on increasing Gr from 1.86 × 10^5 to 8.64 × 10^5 and is about 50 to 60% depending upon the clearance value.
- Further, present findings highlight the effect of increased dimensionless fin spacing from 0.2 to 0.5 at Gr = 4.42 × 10^5 increase in overall Nu is maximum of about 90%. Particularly at S^* = 0.3, the local Nu observed to be increased by 150 %, when Gr value is increased by about 3.65 times.
- Finally, a correlation for overall Nu is developed and valid for a range of $1.86\times10^5 \le Gr \le 8.64\times10^5$, $0.2 \le S^* \le 0.5$, and $0.05 \le C^* \le 0.50$.

REFERENCES

Al-Sarkhi, A., E. Abu-Nada, B. A. Akash and J. O. Jaber (2003). Numerical investigation of shrouded fin array under combined free and forced convection, Int. Comm. *Heat Mass Transf* 30, 435-444.

Arquis, E. and Md. Rady (2005), Study of natural convection heat transfer in a finned horizontal fluid layer. *International Journal of Thermal Sciences* 44, 43-52.

Chang, S. W., H. W. Wub, D. Y. Guob, J. J. Shi and T. H. Chen (2017). Heat transfer enhancement of vertical dimpled fin array in natural convection. *International Journal of Heat and Mass Transf.*, 106, 781–792.

Das, B. and A. Giri (2014). Non-Boussinešq laminar mixed convection in a non-isothermal fin array. *Applied Thermal Engineering* 63, 447–458.

Das, B. and A. Giri (2015). Mixed convective heat transfer from vertical fin array in the presence of vortex generator. *International Journal of Heat and Mass Transfer* 82, 26–41.

Dialameh, L., M. Yaghoubi and O. Abouali (2008). Natural convection from an array of horizontal rectangular thick fins with short length. *Applied Thermal Engineering* 28, 2371–2379.

Dogan, M. and M. Sivrioglu (2012). Experimental and numerical investigation of clearance gap effects on laminar mixed convection heat transfer from fin array in a horizontal channel-A conjugate analysis. *Applied Thermal Engineering* 40, 102-113.

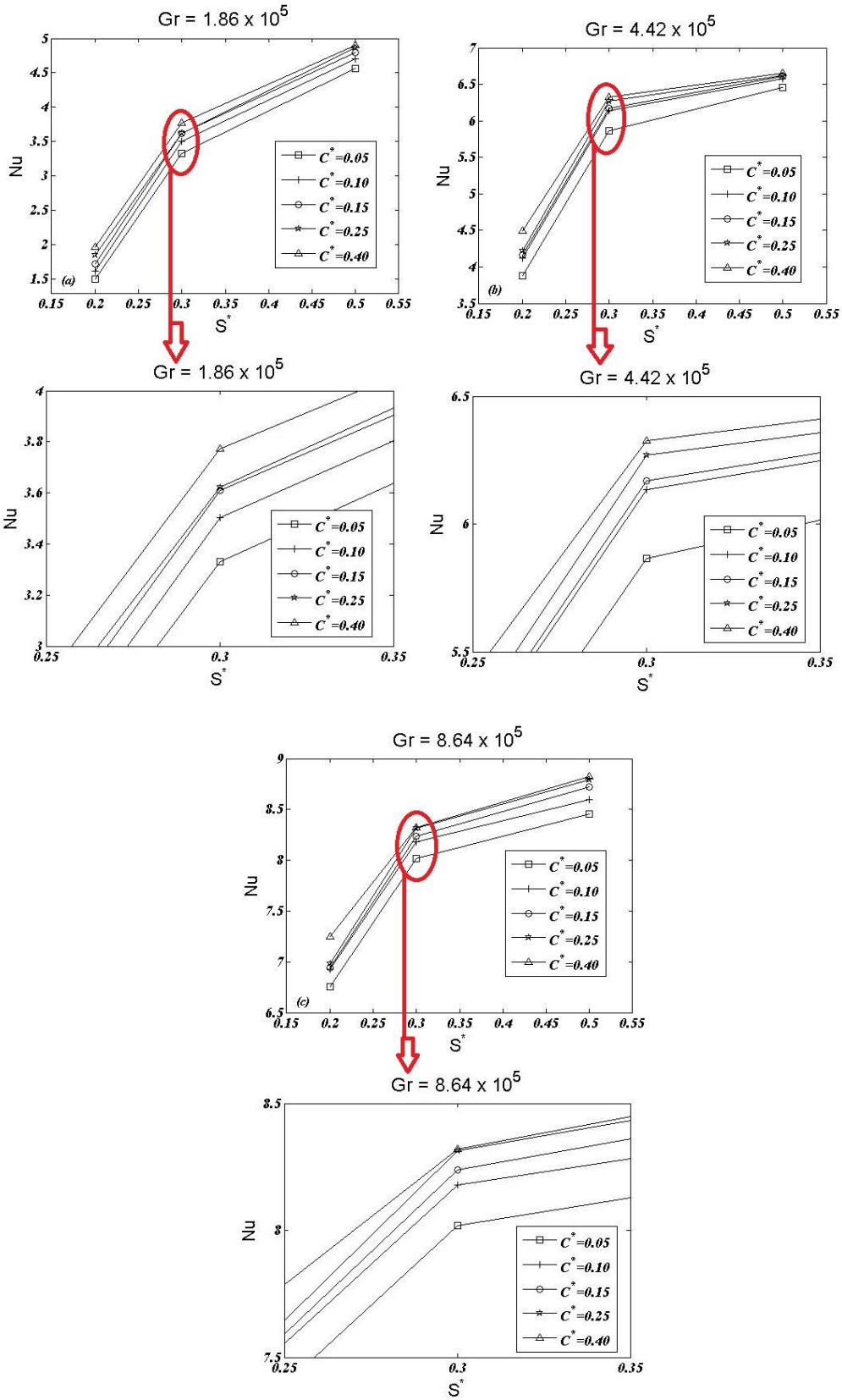

Fig. 11. Variation of overall Nusselt number at (a) Gr = 1.86 x 10^5, (b) Gr = 4.42 x 10^5 and (c) Gr = 8.64 x 10^5 along with maginfied plot.

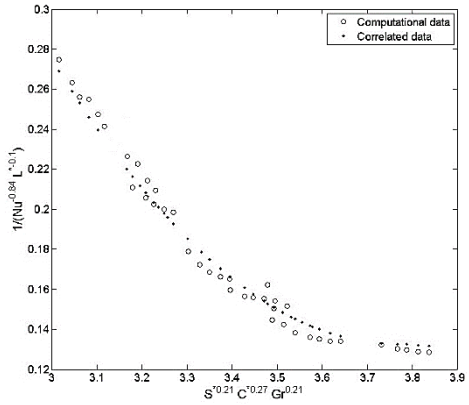

Fig. 12. Plot of correlated data for overall Nusselt number.

Emery, A. F. and J. W. Lee (1999). The Effects of Property Variations on Natural Convection in a Square Enclosure. *Journal of Heat Transfer* 121, 57-62.

Feng, S., M. Shi, H. Yan, S. Sun, F. Li and T. J. Lu (2018). Natural convection in a cross-fin heat sink. *Applied Thermal Engineering* 132, 30–37.

Fisher, T. S. and K. E. Torrance (1999). Experiments on chimney-enhanced free convection. *Trans. ASME, Journal of Heat Transfer* 121, 603–609.

Giri, A. and B. Das (2012). A numerical study of entry region laminar mixed convection over shrouded vertical fin arrays. *International Journal of Thermal Sciences* 60, 212-224.

Goshayeshi, H. R, M. Fahiminia and Md. M. Naserian (2011). Improvement of Free Convection Heat Transfer Rate of Rectangular Heatsink on Vertical Base Plates. *Energy and Power Engineering* 3, 525-532.

Guvenc, A. and H. Yuncu (2001). An experimental investigation on performance of fins on a horizontal base in free convection heat transfer. *Heat Mass Transfer* 37, 409-416.

Haghighi, S. S., H. R. Goshayeshi and Md. R. Safaei (2018). Natural convection heat transfer enhancement in new designs of plate-fin based heat sinks. *International Journal of Heat and Mass Transfer* 125, 640–647.

Harahap, F. and H. N. McManus (1967). Natural convection heat transfer from horizontal rectangular fin arrays. *Journal of Heat Transfer* 89, 32–38.

Huang, G. J. and S. C. Wong (2012). Dynamic characteristics of natural convection from horizontal rectangular fin arrays. *Applied Thermal Engineering* 42, 81-89.

Karki, K. C. and S. V. Patankar (1987). Cooling of a vertical shrouded fin array by natural convection: a numerical study. *Journal of Heat Transfer* 109, 671–676.

Lee, M., H. J. Kim and D. K. Kim (2016). Nusselt number correlation for natural convection from vertical cylinders with triangular fins. *Applied Thermal Engineering* 93, 1238–1247.

Leung, C. D., S. D. Probert and M. J. Shilston (1985). Heat exchangers: Optimal separation for vertical rectangular fins protruding from a vertical rectangular base. *Applied Energy* 19, 77–85.

Li, Z., X. Huai, Y. Tao and H. Chen (2007). Effects of thermal property variations on the liquid flow and heat transfer in microchannel heat sinks. *Applied Thermal Engineering* 27, 2803–2814.

Patankar, S. V. (1980). *Numerical Heat Transfer and Fluid Flow*, Hemisphere, Washington, DC.

Pathak, K. K., A. Giri and P. Lingfa (2018). A numerical study of natural convective heat transfer from a shrouded vertical variable height non-isothermal fin array *Applied Thermal Engineering* 130, 1310–1318

Reddy, P. V., G. S. V. L. Narasimham, S. V. R. Rao, T. Johny and K. V. Kasiviswanathan (2010). Non-Boussinésq conjugate natural convection in a vertical annulus. *International Communications in Heat and Mass Transfer* 37, 1230–1237.

Starner, K. E. and H. N. McManus (1963). An experimental investigation of free-convection heat transfer from rectangular-fin arrays. *Journal of Heat Transfer* 85, 273–278.

Welling, J. R. and C. V. Wooldridge (1965). Free convection heat transfer coefficients from rectangular vertical fins. *Journal of Heat Transfer* 87, 439–444.

Yazicioglu, B. and H. Yuncu, (2007). Optimum fin spacing of rectangular fins on a vertical base in free convection heat transfer. *Heat Mass Transfer* 44, 11–21.

Yüncü, H. and G. Anbar (1998). An experimental investigation on performance of rectangular fins on horizontal base in free convection heat transfer. *Heat Mass Transfer* 33, 507-514.

Zhang, Y. and Y. Cao (2018), A numerical study on the non-Boussinesq effect in the natural